Published in final edited form as:

Circulation. 2018 December 11; 138(24): 2809–2816. doi:10.1161/CIRCULATIONAHA.118.034886.

Regenerative Potential of Neonatal Porcine Hearts

Wuqiang Zhu, MD, PhD[1,#], **Eric Zhang, BS**[1], **Meng Zhao, MD**[1], **Zechen Chong, PhD**[2], **Chengming Fan, MD**[1], **Yawen Tang, BS**[1], **Jervaughn D. Hunter, BS**[1], **Anton V. Borovjagin, PhD**[1], **Gregory P. Walcott, MD**[1], **Jake Y. Chen, PhD**[3], **Gangjian Qin, MD**[1], and **Jianyi Zhang, MD, PhD**[1,#]

[1]School of Medicine and School of Engineering, the University of Alabama at Birmingham, Birmingham, AL 35294, USA

[2]Department of Genetics, School of Medicine, University of Alabama at Birmingham, AL 35294, USA

[3]Informatics Institute, School of Medicine, University of Alabama at Birmingham, AL 35294, USA

Abstract

Background: Rodent hearts can regenerate myocardium lost to apical resection or myocardial infarction for up to 7 days after birth, but whether a similar window for myocardial regeneration also exists in large mammals is unknown.

Methods: Acute myocardial infarction (AMI) was surgically induced in neonatal pigs on postnatal days 1, 2, 3, 7, and 14 (i.e., the P1, P2, P3, P7, and P14 groups, respectively). Cardiac systolic function was evaluated before AMI and at 30 days post AMI via transthoracic echocardiography. Cardiomyocyte cell cycle activity was assessed via immunostaining for proliferation and mitosis markers, infarct size was evaluated histologically, and telomerase activity was measured by quantitative PCR.

Results: Systolic function at day 30 post- AMI was largely restored in P1 animals and partially restored in P2 animals, but significantly impaired when AMI was induced on postnatal day 3 or later. Hearts of P1 animals showed little evidence of scar formation or wall thinning on day 30 after AMI, with increased measures of cell-cycle activity seen six days after AMI (i.e. postnatal day 7) compared to postnatal day 7 in noninfarcted hearts.

Conclusion: The neonatal porcine heart is capable of regeneration following AMI during the first 2 days of life. This phenomenon is associated with induction of cardiomyocyte proliferation, and is lost when cardiomyocytes exit cell cycle shortly after birth.

Keywords

heart; cell cycle; regeneration; neonates; porcine

[#]**Corresponding author** Jianyi (Jay) Zhang, MD, PhD, Department of Biomedical Engineering, School of Medicine and School of Engineering, The University of Alabama at Birmingham, 1720 2nd Ave S, VH G094J, Birmingham, AL 35294-0019, Telephone: 205-934-8421, jayzhang@uab.edu. Wuqiang Zhu, MD, PhD, Department of Biomedical Engineering, School of Medicine, School of Engineering, The University of Alabama at Birmingham, 1720 2nd Ave S, VH G094E, Birmingham, AL 35294-0019, Tel: 205-934-0228, Fax: 205-934-9101, wzhu@uab.edu.

DISCLOSURES

None.

INTRODUCTION

Heart failure is a costly and deadly disease that affects over 20 million patients worldwide, including 5 million Americans. The inability of the adult mammalian heart to regenerate cardiomyocytes following cardiac injury is the primary underpinning of cardiomyopathy. However, in sharp contrast to the hearts of adult mammals, neonatal murine hearts are capable of complete regeneration following either apical resection or myocardial infarction without significant hypertrophy or fibrosis.[1, 2] This regenerative response is mediated via proliferation of the remaining uninjured cardiomyocytes, which is lost by postnatal day 7, when murine cardiomyocytes exit the cell cycle. Thus, myocardial infarctions that occur after postnatal day 7 in mice result in a large fibrotic scar and left-ventricular (LV) contractile dysfunction.

Interestingly, observational studies suggest that the newborn human heart may also be able to mount a regenerative response in the early postnatal window[3–5], although these reports are observational and do not distinguish between contractile dysfunction and true cardiomyocyte loss. Nevertheless, these observations suggest the human heart may be capable of regenerating via proliferation of pre-existing cardiomyocytes for a short period following birth. If so, hearts of other large mammals likely possess similar regenerative potential, and experiments in such large-mammal models would allow for deciphering of the mechanisms which support myocardial regeneration (e.g., myocyte proliferation, stem cell differentiation, or a combination of the two), with significant therapeutic implications for patients suffering from congestive heart failure. As such, the present study was carried out to determine whether neonatal porcine hearts are capable of regeneration, and if so, to define the duration of the postnatal regenerative window, characterize the extent of the regenerative capacity, and identify the cellular source responsible for myocardial regeneration. Our results indicate that porcine hearts possess significant regenerative capacity within the first 2 days after birth, a capability which we found to be attributable to cardiomyocyte proliferation, and significantly attenuated in the days following thereafter.

MATERIALS AND METHODS

The data that support the findings of this study are available from the corresponding authors to other researchers upon reasonable request.

Animals

All experimental protocols were approved by The Institutional Animal Care and Use Committee (IACUC) of the University of Alabama at Birmingham and performed in accordance with the National Institutes of Health Guide for the Care and Use of Laboratory Animals (NIH publication No 85–23).

Feeding and total number studied—Prestage farm pigs at various ages (P1, P2, P3, P7, P14, and P31–44) were purchase from Prestage Farm Inc (West Point, MS). All pigs younger than P14 were housed at incubator at a temperature of ~85 ^{0}F and room air. Piglets were fed with bovine colostrum every 4 hours for the first 2 days of life, 1:1 colostrum/sow's

milk at day 3 of life, and sow's milk thereafter. Animals were given supplemental iron at day 7. A total of 56 pigs were included in this study. Among these, 36 pigs received open chest surgery, and the other 20 pigs without surgery were used as control (normal). Five pigs died within 7 days after surgical procedure.

Surgical procedure—AMI was induced via permanent ligation of the left descending coronary artery on postnatal day 1, 2, 3, 7, and 14 (i.e., the P1, P2, P3, P7, and P14 groups, respectively), as described previously.[6] Briefly, pigs were anesthetized with isoflurane and placed in a dorsal recumbent position on a heating pad, a median sternotomy was performed to expose the heart, and the left anterior descending coronary artery distal to the 2nd diagonal was ligated by a ligature; then, the sternum was re-approximated, the chest was closed in layers, and air was evacuated from the mediastinum. After surgery, the animals were maintained in a temperature-controlled incubator until old enough to maintain their own body temperature.

Echocardiography

Cardiac function was assessed immediately before surgery and at 7 and 30 days afterward via transthoracic echocardiography. Briefly, animals were sedated with isoflurane and placed in a dorsal recumbent position, and then left-parasternal two-dimensional and M-mode echocardiographic images were obtained. Fractional shortening (FS) was measured from short-axis M-mode images at the level of the papillary muscles and parasternal long-axis B-Mode images and then calculated as the difference in left-ventricular (LV) internal dimension during diastole and systole (LVIDd and LVIDs, respectively) divided by the LVIDd and expressed as a percentage (FS = [LVIDd – LVIDs] / LVIDd × 100%). Systolic and diastolic wall thicknesses were measured from the apical short-axis view. In hearts with post-infarction LV remodeling, LV scar bulging (systolic thinning) characterizes the severity of LV dilatation. Changes of LV anterior wall systolic thickening/thinning over time was calculated at baseline and 30 days after AMI. Because animals were studied at different postnatal ages (ranging from P1 to P14), we normalized changes of anterior wall thickness to baseline value (before the AMI) of each heart. LV anterior wall systolic thickening/ thinning was calculated using the following formula:

$$\textbf{Delta THs \%} = \left[\left(\textbf{delta Th}_{\textbf{D30}} - \textbf{delta Th}_{\textbf{BL}}\right) \times \textbf{100 \%}\right] / \textbf{delta Th}_{\textbf{BL}}$$

Where Delta TH_S % indicates LV systolic thickening, BL denotes baseline, and changes of anterior wall thickness $\textbf{(delta Th}_{\textbf{Dx}}\textbf{)} = \textbf{sTh}_{\textbf{Dx}} - \textbf{dTh}_{\textbf{Dx}}$, where the sTh_{Dx} and dTh_{Dx} represents systolic and diastolic anterior wall thickness (mm) at post AMI Day x, respectively.

Histology

Hearts were cut into transverse blocks (thickness: 1 cm), and myocardium from the infarcted zone (IZ) and the zone bordering the infarct (BZ) were either snap frozen with liquid nitrogen or processed with 10% formalin and 30% sucrose overnight. Samples were cut into transverse sections (thickness: 10 μm) and stained with antibodies against Ki67,

phosphorylated histone 3 (PH3), Nkx2.5, and cardiac troponin T (cTnT) (Supplemental Table I); then, positively stained cells were counted in at least 3 sections per heart (with 12 high power of fields in each section), normalized to the total number of cardiomyocytes, and expressed as a percentage. For each animal, at least 3 sections of border zone myocardium were analyzed, and a total of 12 images from subendomyocardium, midmyocardium, and subepimyocardium were counted. To evaluate infarct area, heart sections from the IZ and part of the BZ of the LV and septum were fixed in Bouin's solution and stained with sirius red (scar tissue) and fast green (myocardial tissue). Images were obtained with a dissection scope.

Telomerase activity assay

Telomerase activity was measured in tissue extracts using the TRAPeze RT Telomerase Detection Kit (Millipore Cat #S7710). Briefly, small pieces of heart tissue were homogenized in CHAPS lysis buffer, sonicated, and centrifuged at 7000 g for 5 min; the supernatants were collected, and protein concentrations were determined with the BCA method (Pierce Company) and adjusted to 0.5 μg/μL. For each assay, the mixture was composed of 5' TRAPeze RT Reaction Mix (4 μL), PCR-grade water (13.6 μL), TITANIUM Taq DNA Polymerase (0.4 μL), and the tissue extract or control template (2 μL). Reactions were performed in triplicate, and PCR was performed in an Applied Biosystems 7300 Real-Time PCR system via the following protocol: 30 min at 30 °C (extension of telomerase substrate), 2 min at 95 °C, and then 45 cycles consisting of 15 sec at 94 °C, 1 min at 59 °C, and 30 sec at 45 °C (PCR amplification of extended telomerase substrate).

RNA sequencing

It was previously reported that the regenerative state of cardiomyocytes in neonatal mice is associated with microenvironmental factors such as inflammation, fibrosis, and angiognesis.[7–9] Accordingly, studies of unbiased deep RNA sequencing were done on myocardium of P1, P3, and P14 group hearts at Day 30 post AMI (see Online Supplement).

Statistics

Data are presented as mean ± SEM, and each in-vitro experiment was performed at least three times. Statistical analysis was performed by using GraphPad Prism 7 and SigmaStat 4.0 software. Comparisons between groups were evaluated via one-way analysis of variance (ANOVA) (all figures except Figure 1C) or via repeated measures two-way ANOVA (Figure 1C) followed by the Holm-Sidak test for multiple comparisons. $P<0.05$ was considered significant.

RESULTS

Myocardial regeneration in neonatal pigs

AMI was surgically induced via distal left anterior descending (LAD) coronary artery ligation (distal to the 2nd diagonal) in animals on postnatal days 1, 2, 3, 7, and 14 (i.e., the P1, P2, P3, P7, and P14 groups, respectively), and transthoracic echocardiography (Figure 1A) was performed to assess wall thickness and cardiac function. P1 animals were sacrificed 6, 13, or 30 days after AMI, and animals in groups P2-P14 were sacrificed 30 days after

AMI. LV anterior wall systolic thickening at Day 30 post AMI is illustrated on Figure 1 Panels A to B. The LV anterior wall systolic thickening/thinning at Day 30 post AMI are presented as Delta THs % (Delta TH_s % indicates LV systolic thickening). A progressively more severe LV systolic thinning occurred in P3, P7, and P14 age group of neonate pigs at Day 30 post AMI, which did not occur in P1 and P2 group animals (Figure 1B). At Day 30 post AMI, post mortem evaluation of LV anterior wall thickness was similar among the groups of control, P1 and P2 group hearts (Figure 1, Panels D-E). Furthermore, measurements of fractional shortening indicated that cardiac function had completely recovered by Day 30 post AMI in P1 animals, but not in P3, or P14 animals (Figure 1C). The sections from the hearts of P1 animals on postinfarction day 30 displayed little or no evidence of scarring or LV wall thinning (Figure 1D and 1F) when compared to sections from P14 animals. P2 group animals with LAD ligation also tended to maintain the LV anterior wall thickness and showed LV functional recovery similar to the P1 group of animals (Figure 1, Panels B-C). However, the improvement tended to be smaller.

Cardiomyocyte cell cycle activity in normal and injured neonatal pigs

Cardiomyocyte cell-cycle activity was evaluated by staining sections for Ki67 (Figures 2A-2B), PH3 (Figures 2C-2D) and Aurora B (Figure 2E-2F), markers for proliferation, mitosis, and cytokinesis, respectively, and evaluating telomerase activity (Figure 2G). Cardiomyocytes which have exited the cell cycle typically have shorter telomeres.[10] Cardiomyocytes were visualized with anti-cTnT antibodies, and nuclei were labeled with anti-Nkx2.5 antibodies. In normal (i.e., noninfarcted) hearts, the proportion of cardiomyocytes that expressed Ki67 (Figure 2B), PH3 (Figure 2D) or Aurora B (Figure 2F) declined by ~40% between postnatal days 1 and 2, and continued to decrease through postnatal day 45, while telomerase activity gradually declined from postnatal day 1 through postnatal day 31 (Figure 2G). Notably, the proportion of cardiomyocytes that expressed Ki67 (Figure 2B), PH3 (Figure 2D) or Aurora B (Figure 2F) on postnatal day 7 was greater in P1 animals than in normal animals (Ki67: 1.82% in P1 hearts, 0.74% in normal hearts, $p<0.05$; PH3: 0.89% in P1 hearts, 0.43% in normal hearts, $p<0.05$; Aurora B: 0.78% in P1 hearts, 0.23% in normal hearts, $p<0.05$), and the proportion of $Ki67^+$ cardiomyocytes, but not $PH3^+$ cardiomyocytes, remained higher in P1 hearts than in normal hearts on postnatal day 14 (Ki67: 1.39% in P1 hearts, 0.37% in normal hearts, $p<0.05$; PH3: 0.33% in P1 hearts, 0.27% in normal hearts, $p>0.05$). Thus, during the first day after birth, cardiomyocytes in porcine hearts appear capable of responding to AMI by entering the cell cycle and proliferating. It was reported that cardiomyocyte regenerative state in the neonatal mice is associated with microenvironment such as inflammation, fibrosis, and angiognesis.[7–9] In agreement with these reports, our data from unbiased deep RNA sequencing on P1, P3, and P14 pig hearts identified the enrichment of important pathways for cell survival, proliferation, growth, metabolism, and angiogenesis (Supplemental Table II, Supplemental Figure I A-F).

DISCUSSION

Cardiomyocytes in mammals lose their proliferative capacity within the first week of life. However, the neonatal mouse heart was shown to completely recover from injury in the first

few days of life.[1, 2] To date, it is unclear whether a similar phenomenon occurs in large mammals, which would have significant therapeutic implications. The gap of knowledge between the regenerative capacity of cardiomyocytes in response to injury in small and large animals is substantial—whether this regeneration of heart muscle occurs via the differentiation of stem cells, proliferation of pre-existing myocytes, or a combination of both, remains unknown. Furthermore, despite the significant mortality associated with heart failure, a disease responsible for ~280,000 deaths per year,[11] whether cardiomyocytes in neonatal humans or large mammals retain this regenerative potential observed in neonatal rodents remains largely unexplored. The present study demonstrates that the regenerative capacity of cardiomyocytes in porcine hearts remains significant for less than three days after birth. The regenerative capability of P1 porcine hearts was sufficient to completely restore the myocardium and preserve systolic function, while hearts of P2 animals displayed some regenerative potency but not enough to restore normal cardiac function. Intriguingly, a recent report indicates that the regenerative capacity in neonatal mice may also be restricted to the first two days of life[12], suggesting that this phenomenon closely resembles the neonatal heart regeneration seen in rodents. We also observed a rapid decline of cardiomyocyte cell cycle activity, accompanied by a decline in telomerase activity, within 2 weeks after birth, consistent with previous reports that cardiomyocytes that have exited the cell cycle typically have shorter telomeres.[10] Although our data suggested that the cardiac regeneration observed in P1 animals may be largely attributable to the proliferation of pre-existing cardiomyocytes, technical limitations, such as the inability to track cell lineages in current porcine models, preclude us from ruling out at least some contribution from stem cell-mediated myogenesis or other potential mechanisms. In conclusion, our data indicate that porcine hearts retain a remarkable regenerative capacity for a very short period (1–2 days) after birth, and that the regenerative mechanism includes the proliferation and renewal of pre-existing cardiomyocytes.

Supplementary Material

Refer to Web version on PubMed Central for supplementary material.

ACKNOWLEDGEMENT

The authors would like to thank Dr. Yanwen Liu for excellent technical assistance.

SOURCES OF FUNDING

This study is supported by National Institute of Health, National Heart, Lung and Blood Institute RO1 grants HL95077, HL114120, HL131017, HL138023, and UO1 HL134764 (to JZ), an American Heart Association Scientist Development Grant 16SDG30410018 (to WZ).

REFERENCES

1. Porrello ER, Mahmoud AI, Simpson E, Hill JA, Richardson JA, Olson EN and Sadek HA. Transient regenerative potential of the neonatal mouse heart. Science 2011;331:1078–1080. [PubMed: 21350179]
2. Porrello ER, Mahmoud AI, Simpson E, Johnson BA, Grinsfelder D, Canseco D, Mammen PP, Rothermel BA, Olson EN and Sadek HA. Regulation of neonatal and adult mammalian heart regeneration by the miR-15 family. Proc Nat Acad Sci 2013;110:187–192. [PubMed: 23248315]

3. Huddleston CB, Balzer DT and Mendeloff EN. Repair of anomalous left main coronary artery arising from the pulmonary artery in infants: long-term impact on the mitral valve. Ann Thorac Surg 2001;71:1985–8; discussion 1988–1989. [PubMed: 11426779]

4. Ling Y, Bhushan S, Fan Q and Tang M. Midterm outcome after surgical correction of anomalous left coronary artery from the pulmonary artery. J Cardiothorac Surg 2016;11:137. [PubMed: 27562655]

5. Bakhtiary F, Mohr FW and Kostelka M. Midterm outcome after surgical correction of anomalous left coronary artery from pulmonary artery. World J Pediatr Congenit Heart Surg 2011;2:550–553. [PubMed: 23804466]

6. Xiong Q, Ye L, Zhang P, Lepley M, Tian J, Li J, Zhang L, Swingen C, Vaughan JT, Kaufman DS and Zhang J. Functional consequences of human induced pluripotent stem cell therapy: myocardial ATP turnover rate in the in vivo swine heart with postinfarction remodeling. Circulation 2013;127:997–1008. [PubMed: 23371930]

7. Aurora AB, Porrello ER, Tan W, Mahmoud AI, Hill JA, Bassel-Duby R, Sadek HA and Olson EN. Macrophages are required for neonatal heart regeneration. J Clin Invest 2014;124:1382–1392. [PubMed: 24569380]

8. Quaife-Ryan GA, Sim CB, Ziemann M, Kaspi A, Rafehi H, Ramialison M, El-Osta A, Hudson JE and Porrello ER. Multicellular Transcriptional Analysis of Mammalian Heart Regeneration. Circulation 2017;136:1123–1139. [PubMed: 28733351]

9. O'Meara CC, Wamstad JA, Gladstone RA, Fomovsky GM, Butty VL, Shrikumar A, Gannon JB, Boyer LA and Lee RT. Transcriptional reversion of cardiac myocyte fate during mammalian cardiac regeneration. Circ Res 2015;116:804–815. [PubMed: 25477501]

10. Oh H, Taffet GE, Youker KA, Entman ML, Overbeek PA, Michael LH and Schneider MD. Telomerase reverse transcriptase promotes cardiac muscle cell proliferation, hypertrophy, and survival. Proc Natl Acad Sci U S A 2001;98:10308–10313. [PubMed: 11517337]

11. Writing Group M, Mozaffarian D, Benjamin EJ, Go AS, Arnett DK, Blaha MJ, Cushman M, Das SR, de Ferranti S, Despres JP, Fullerton HJ, Howard VJ, Huffman MD, Isasi CR, Jimenez MC, Judd SE, Kissela BM, Lichtman JH, Lisabeth LD, Liu S, Mackey RH, Magid DJ, McGuire DK, Mohler ER, 3rd, Moy CS, Muntner P, Mussolino ME, Nasir K, Neumar RW, Nichol G, Palaniappan L, Pandey DK, Reeves MJ, Rodriguez CJ, Rosamond W, Sorlie PD, Stein J, Towfighi A, Turan TN, Virani SS, Woo D, Yeh RW, Turner MB, American Heart Association Statistics C and Stroke Statistics S. Executive Summary: Heart Disease and Stroke Statistics−−2016 Update: A Report From the American Heart Association. Circulation 2016;133:447–454. [PubMed: 26811276]

12. Notari M, Ventura-Rubio A, Bedford-Guaus SJ, Jorba I, Mulero L, Navajas D, Marti M and Raya A. The local microenvironment limits the regenerative potential of the mouse neonatal heart. Sci Adv 2018;4:eaao5553. [PubMed: 29732402]

CLINICAL PERSPECTIVES

1. What is new?

- We demonstrate here that hearts of 1-day-old porcine (P1) can functionally and structurally recover from AMI via myocyte proliferation; some evidence of myocardial regeneration via proliferation was also observed in the P2 hearts. Although myocyte cell-cycle activity was detectable in P7 to P44 hearts after AMI, it occurred at much lower levels with no significant structural regeneration or functional recovery.
- In normal hearts, myocyte cell-cycle activity and proliferation were 3-fold higher in P1 than in P7 hearts.
- Measurements of cell-cycle activity were greater in cardiomyocytes in infarcted hearts than normal hearts at same postnatal age.
- In large mammals, AMI activates cell-cycle activity in surviving cardiomyocytes of P1 animals, which subsequently replaced cardiomyocytes lost during injury.

2. What are the clinical implications?

- While it is known that the rodent heart is capable of cardiac regeneration during the first 7 days after birth, whether a similar regenerative window exists in large mammals is unknown. Demonstration of a significant myocardial regeneration window in the early postnatal stage of large mammalian hearts is highly impactful. Our findings provide insight into the regenerative properties of the early postnatal human heart.

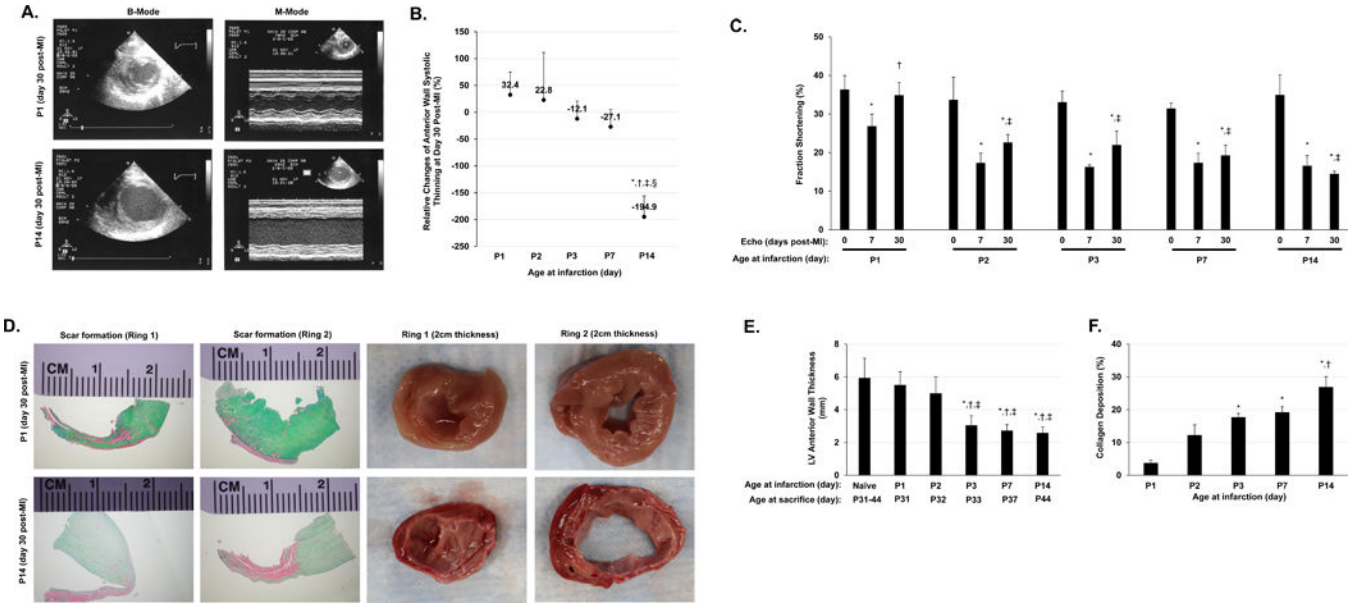

Figure 1. Evaluation of cardiomyocyte regeneration in neonatal porcine hearts.

AMI was surgically induced in neonatal pigs on postnatal days 1, 2, 3, 7, and 14 (i.e., the P1, P2, P3, P7, and P14 groups, respectively). (A) B-Mode and M-Mode images were acquired via transthoracic echocardiography; representative images were displayed for animals in the P1 and P14 groups on day 30 after AMI induction. (B) Echocardiographic images of LV systolic thickening obtained before AMI induction and 30 days afterward were used to calculate the relative change in LV anterior wall systolic thickening/thining. *P<0.05 vs. P1, †P<0.05 vs. P2, ‡P<0.05 vs. P3, §P<0.05 vs. P7. One-way ANOVA with the Holm-Sidak method. n=3–4 animals in each group. (C) Fractional shortening was evaluated before and 30 days after AMI induction. *P<0.05 vs. Pre-AMI (day 0) for the same experimental group; †P<0.05 vs. P1 at day 7 post-AMI; ‡p<0.05 vs. P1 at day 30 post-AMI. Repeated measures two-way ANOVA. n=3–4 animals in each group. (D) LV heart sections from P1 and P14 animals were obtained on day 30 after AMI induction and stained with Sirius red and Fast-green to identify the scarred (red) and unscarred regions, respectively (left four panels) or observed macroscopically (right four panels) to evaluate wall thinning. LV anterior wall thickness (E) and Scar size (as indicated by % collagen deposition in F) were quantified. For (E): *P<0.05 vs. normal hearts of control animals; †p<0.05 vs. P1 AMI animals; ‡P<0.05 vs. P2 AMI animals; for (F): *P<0.05 vs. P1 AMI animals; †p<0.05 vs. P2 AMI animals; One-way ANOVA with the Holm-Sidak method. n=3–4 animals in each group.

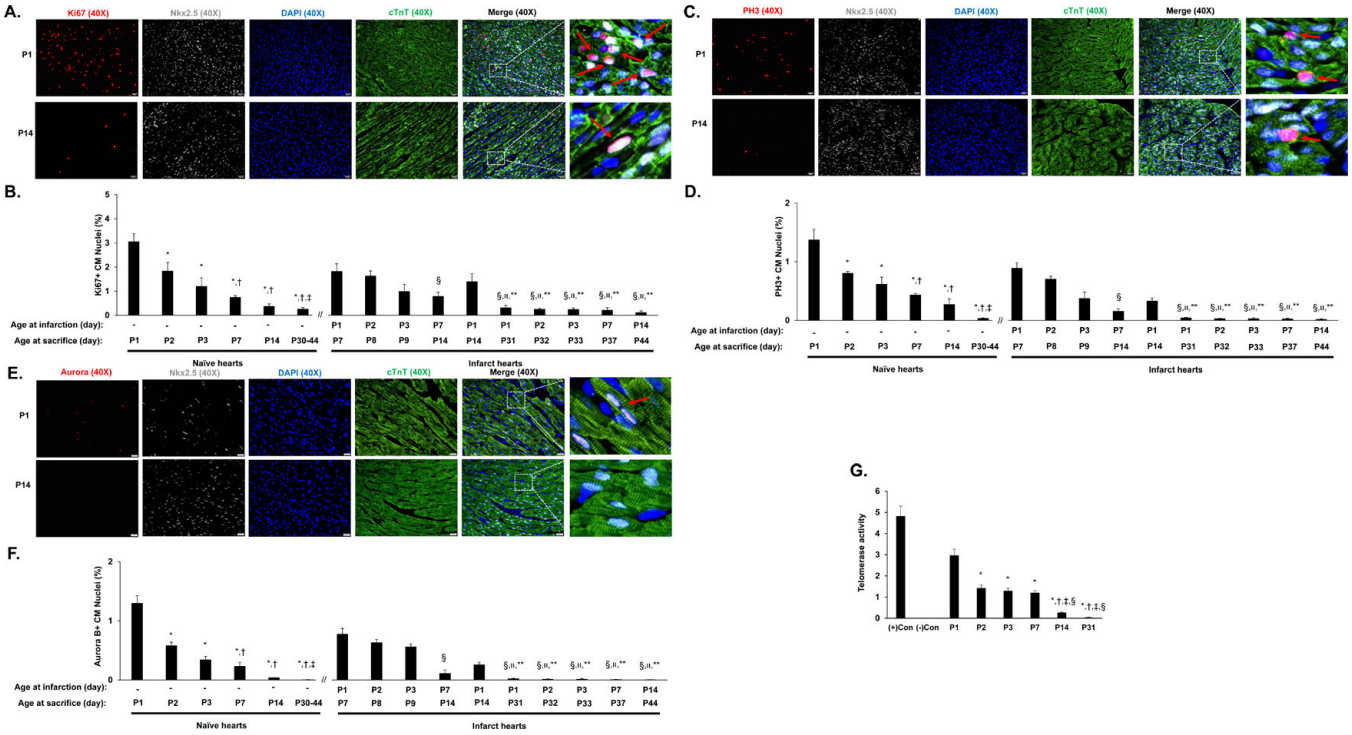

Figure 2. Characterization of cell cycle activity and proliferation in neonatal porcine hearts.

(A-F) The expression of proliferation (Ki67), mitosis (PH3), and cytokinesis (Aurora B) markers was evaluated via immunofluorescent staining in paraformaldehyde-fixed heart sections; cardiomyocytes were visualized by staining for cTnT, and nuclei were labeled with anti-Nkx2.5 antibodies and counter-stained with DAPI. Cardiomyocytes that stained positively for each marker (Ki67, PH3, or Aurora B) were counted, normalized to the total number of cardiomyocytes (Nkx2.5-cTnT double-positive cells) and expressed as a percentage. A total of 3 sections of border zone myocardium (12 images) were counted. (A) Representative images are displayed for sections used to evaluate Ki67 expression on in the normal hearts of P1 and P14 animals (Bar = 20 μm) (B) Cardiomyocyte proliferation was quantified at the indicated day of sacrifice in normal hearts and in the AMI hearts of P1, P2, P3, P7, and P14 animals as the proportion of Nkx2.5-cTnT double-positive cells that also expressed Ki67. The data for days P30-P44 were pooled. *P<0.05 vs. P1 normal hearts; †P<0.05 vs. P2 normal hearts; ‡P<0.05 vs. P3 normal hearts; §P<0.05 vs. P1 AMI hearts (harvested at P7); ⁋P<0.05 vs. P2 AMI hearts (harvested at P8); **P<0.05 vs. P1 AMI hearts (harvested at P14). One-way ANOVA with the Holm-Sidak method. n=3–4 animals in each group. (C) Representative images are displayed for sections used to evaluate PH3 expression in the hearts of P1 and P14 normal animals (Bar = 20 μm). (D) Cardiomyocyte mitosis was quantified at the indicated day of sacrifice in normal hearts and in the AMI hearts of P1, P2, P3, P7, and P14 animals as the proportion of Nkx2.5-cTnT double-positive cells that also expressed PH3. The data for days P30-P44 were pooled. *P<0.05 vs. P1 normal hearts; †P<0.05 vs. P2 normal hearts; ‡P<0.05 vs. P3 normal hearts; §P<0.05 vs. P1 AMI hearts (harvested at P7); ⁋P<0.05 vs. P2 AMI hearts (harvested at P8); **P<0.05 vs. P1 AMI hearts (harvested at P14). One-way ANOVA with the Holm-Sidak method. n=3–4 animals in each group. (E) Representative images are displayed for sections used to evaluate Aurora B

expression in the hearts of P1 and P14 normal animals (Bar = 20 μm). (F) Cardiomyocyte cytokinesis was quantified at the indicated day of sacrifice in normal hearts and in the AMI hearts of P1, P2, P3, P7, and P14 animals as the proportion of Nkx2.5-cTnT double-positive cells that also expressed PH3. The data for days P30-P44 were pooled. *P<0.05 vs. P1 normal hearts; †P<0.05 vs. P2 normal hearts; ‡P<0.05 vs. P3 normal hearts; §P<0.05 vs. P1 AMI hearts (harvested at P7); ⁋P<0.05 vs. P2 AMI hearts (harvested at P8); **P<0.05 vs. P1 AMI hearts (harvested at P14). One-way ANOVA with the Holm-Sidak method. n=3–4 animals in each group. (G) Telomerase activity was assessed in the myocardium of normal hearts on postnatal days 1, 2, 3, 7, 14, and 31 (P1, P2, P3, P7, P14, and P31, respectively). Control assessments were performed with (+) or without (−) telomerase which were included in the kit. *P<0.05 vs. P1; †P<0.05 vs. P2; ‡P<0.05 vs. P3; §P<0.05 vs. P7. One-way ANOVA with the Holm-Sidak method. Experiments were repeated twice (n=3).